Intermetallics 25 (2012) 42–47

Contents lists available at SciVerse ScienceDirect

Intermetallics

journal homepage: www.elsevier.com/locate/intermet

Structure and magnetic properties of $Ni_2(Mn,Co)Ga$ Heusler alloys rapidly solidified by melt-spinning

R.V.S. Prasad [a], M. Manivel Raja [b], G. Phanikumar [a,*]

[a] Department of Metallurgical and Materials Engineering, Indian Institute of Technology Madras, Chennai 600036, India
[b] Advanced Magnetic Materials Group, Defence Metallurgical Research Laboratory, Hyderabad 500058, India

ARTICLE INFO

Article history:
Received 12 October 2011
Received in revised form
6 February 2012
Accepted 17 February 2012
Available online 15 March 2012

Keywords:
A. Magnetic intermetallics
B. Phase identification
C. Rapid solidification processing
D. Microstructure
E. Phase stability

ABSTRACT

In this study microstructure and magnetic properties of cobalt substituted Ni_2MnGa based ferromagnetic shape memory alloys (FMSA) are presented. $Ni_{50}Mn_{(25-x)}Co_xGa_{25}$ (x = 2, 5, 8, 11 at%) alloys were synthesized using the melt-spinning technique. Martensite, austenite and pre-martensitic tweed structures were found at room temperature for alloys containing 2, 5, 8 and 11% Co and melt-spun at two extreme wheels speeds viz., 20 m/s and 30 m/s. However, the alloy containing 5% Co melt-spun at a wheel speed of 20 m/s consists of 7 M or 14 layered Martensite phase. Magnetic properties such as saturation magnetization (Ms), martensitic transformation temperature (T_m) and Curie temperature (T_c) were measured and were found to be attractive for most of the melt-spun alloys containing higher "Co" concentrations. Upon annealing at 1273 K for 1 h, γ (gamma) phase was found to stabilize. The magnetic properties were found to correlate with the phase content of the Co substituted alloys.

1. Introduction

The research on Ni_2MnGa Ferromagnetic shape memory alloys is intense during last decade owing to their application as a potential material in the field of sensors and actuators [1,2]. Alternatives to the Ni_2MnGa alloy, such as Ni–Fe–Ga, Co–Ni–Ga, Ni–Co–Ga, Ni–Co–Al, Ni–Mn–In and Ni–Mn–Sn with an ordered bcc B2-type or $L2_1$- type structure were explored in the recent past [3–8]. Alloying additions to replace manganese and gallium are being explored for several reasons including improving the ductility and avoiding excessive vaporization loss of elements during processing [9,10]. Earlier researchers reported most of the work on arc-melted Ni–Mn–Co–Ga samples and annealing followed by quenching. These studies revealed that cobalt addition to Ni_2MnGa alloys leads to giant magneto caloric effect, increase in ductility, and enhancement of magnetic properties [11–18]. However, open literature on the phase content and magnetic properties of $Ni_2(Mn,Co)Ga$ Heusler alloys synthesized by melt spinning are limited.

Rapid solidification of $Ni_2(Mn,Co)Ga$ based alloys can take advantage of extended solid solution formation and metastable microstructures to explore interesting magnetic properties. Studies on Ni_2MnGa and derived alloys revealed formation of martensite, nano-crystalline and amorphous phases and the magnetic properties are observed to be strongly correlated to the constituent phases in the sample [19–22]. In this study, cobalt substitution in place of manganese was explored with the objective of bringing the martensite transformation temperature closer to room temperature and also to retain the magnetic properties.

2. Experimental methodology

A series of $Ni_{50}Mn_{(25-x)}Co_xGa_{25}$ (x = 2, 5, 8, 11 at%) alloys were prepared by arc melting 99.99% pure Ni, Mn, Co and Ga in argon atmosphere. These alloys will be referred to by their respective cobalt content (2%-Co etc.). Samples were prepared as 5 g buttons and melted four to five times to ensure homogeneity. A conventional copper wheel was used to melt-spin the alloys under vacuum of 10^{-5} mbar. For each composition, approximately 5 g of alloy was induction melted in a quartz tube that has an orifice of 0.8 mm diameter, and ejected with a 1.10 bar back-pressure of argon gas. Two extreme wheel speeds of 20 m/s and 30 m/s were chosen for each alloy composition after several attempts to achieve a good quality of ribbon with uniform thickness. These speeds will be referred to as high (30 m/s) and low (20 m/s) for brevity. All the melt-spun ribbons were sealed in an evacuated quartz tube and then annealed at 1273 K for 1 h. Microstructure and phase analysis was performed using Transmission Electron Microscopy (TEM) and

* Corresponding author. Tel.: +91 44 2257 4770; fax: +91 44 2257 4752.
E-mail address: gphani@iitm.ac.in (G. Phanikumar).

0966-9795/$ – see front matter © 2012 Elsevier Ltd. All rights reserved.
doi:10.1016/j.intermet.2012.02.012

(Cu-Kα) X-Ray diffraction (XRD). Room temperature magnetic and thermo-magnetic measurements on melt-spun ribbon samples were obtained by vibrating sample magnetometer (VSM).

3. Experimental results

3.1. Microstructure and phase analysis

3.1.1. As-spun ribbons

XRD patterns of all samples melt-spun at low wheel speed shown in Fig. 1a demonstrate phase evolution as function of composition. The 2%-Co alloy samples contain austenite phase with B2 atomic ordering. However, 5%-Co alloy samples could be indexed to 7 M or 14 layered Martensite. Similar patterns have been observed by Pons *et al.* [23] in melt-spun Ni_2MnGa alloys. XRD peaks from 8%-Co and 11%-Co alloys were indexed to martensite phase with non-modulated tetragonal structure. All the peaks were sharp, indicating crystalline nature and absence of amorphous content.

XRD studies on samples melt-spun at high wheel speed show a different phase evolution (Fig. 1b). The peaks correspond to 2%-Co and 5%-Co alloy samples were indexed to austenite phase with B2 ordering and the 8%-Co and 11%-Co alloys were indexed to martensite phase with non-modulated tetragonal structure.

Extensive transmission electron microscopy was performed to confirm the phases and also to determine any minor phases that could have formed during the processing of the alloys. Salient results are presented here. Fig. 2 shows bright field image and corresponding selected area electron diffraction (SAED) pattern of 5%-Co substituted sample. Uniformly distributed grains with an average grain size about 0.5–1.5 μm can be noticed. Corresponding SAED pattern taken along $[04\bar{4}]$ zone axis confirms austenite phase with B2 atomic ordering. Bright field images from different locations of the sample are also shown in the same figure. Pre-martensitic tweed structures can be seen in the Fig. 2c and the same image at higher magnification is shown in Fig. 2d. Tweed structures were observed in a number of alloy systems that undergo martensite transformation [24–28] including Ni_2MnGa [29]. Kartha and co-workers [30,31] have analysed these structures to be disorder driven pre-martensite structures.

TEM bright field images of 8%-Co substituted sample are shown in Fig. 3 in different magnifications. Martensite phase with twins and twin variants can be seen clearly and also indicated in Fig. 3b with arrow marks. The SAED pattern was taken along the [044] zone axis and corresponding reflections have been indexed to martensite phase with non-modulated tetragonal structure.

3.1.2. Annealed ribbons

XRD patterns of ribbons melt-spun at lower wheel speed and annealed at 1273 K for 1 h show that there is a phase evolution during annealing that is characteristic of the cobalt content of the alloy (Fig. 4). The XRD peaks of 2%-Co sample could be indexed to a phase mixture of austenite phase with $L2_1$ Heusler atomic ordering and martensite phase with non-modulated tetragonal structure. However, the 5%-Co and 8%-Co samples are single phase and the respective reflections have been indexed to martensite phase with non-modulated tetragonal structure. The 11%-Co sample indicates precipitation of γ (gamma) phase with f.c.c. structure coexisting with martensite with non-modulated tetragonal structure.

Similarly phase analysis has been performed on annealed samples of ribbons melt-spun at high wheel speed (Fig. 5). The 2%-Co substituted sample confirms to austenite phase with $L2_1$ Heusler atomic ordering. All samples with higher cobalt content (5%, 8% and 11%) have been indexed to a phase mixture of both γ (gamma) with f.c.c. structure and martensite with non-modulated tetragonal structure.

Higher cobalt content and rapid solidification resulted in ordering of B2 phase. However, presence of martensite phase at room temperature and precipitation of γ (gamma) phase depends on the alloy content.

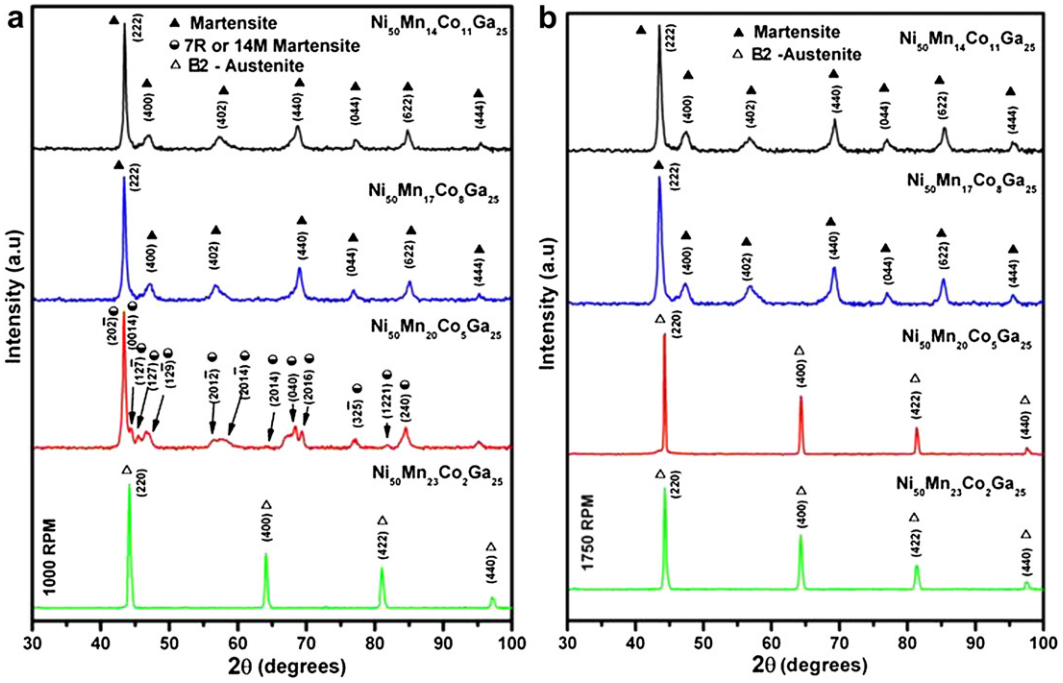

Fig. 1. XRD patterns of $Ni_2(Mn,Co)Ga$ alloy melt-spun at (a) low wheel speed and (b) high wheel speed. Patterns of samples containing cobalt content of 2, 5, 8 and 11% are shown in increasing order from bottom to top.

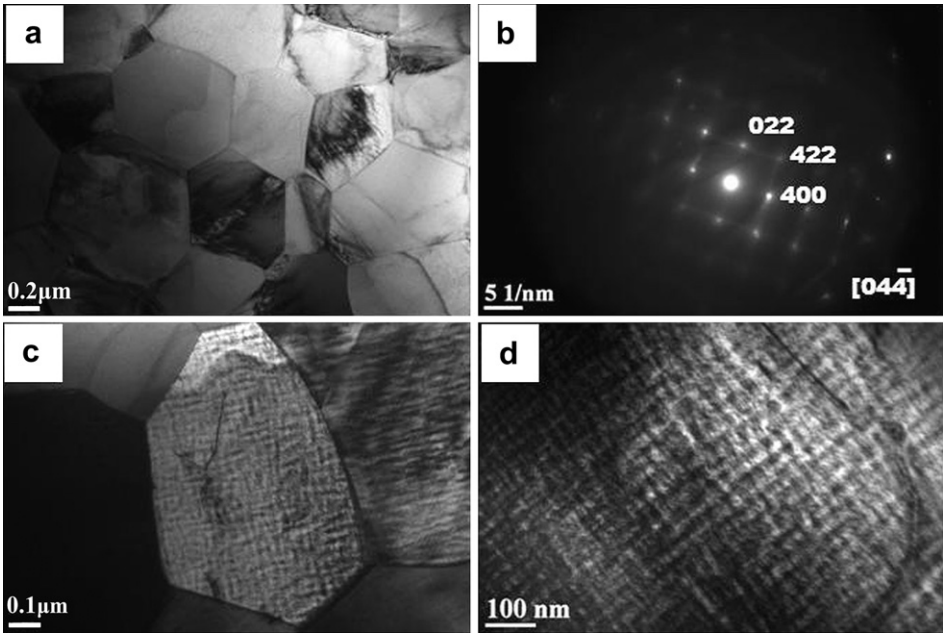

Fig. 2. TEM micrographs of $Ni_{50}Mn_{20}$ Co_5Ga_{25} alloy melt-spun at high wheel speed (a) Bright field image showing austenite phase (b) Corresponding SAED pattern taken from austenite phase has been indexed B2 atomic ordering along [04] zone axis (c) Bright field image shows existence of both austenite and pre-martensitic tweed structure (d) Bright field image of pre-martensitic tweed structure alone at higher magnification.

3.2. Magnetic properties

Magnetic properties such as saturation magnetization (Ms), martensitic transformation temperature (T_m) and Curie temperature (T_c) are measured by utilizing different magnetic characterization tools such as vibrating sample magnetometer and susceptibility meter.

Saturation magnetization as a function of cobalt content (or e/a ratio) is plotted in Fig. 6a and also listed in Table 1. One can note that saturation magnetization of as-spun samples decreases monotonously as the cobalt content is increased. On the other hand, after annealing treatment the magnetization values are decreasing compared to as-spun samples. However, the observed values are good agreement with existing literature as suggested in Fig. 2b in reference [32].

Martensitic transformation temperatures for alloys of different cobalt content and different processing conditions are given in the Fig. 6b and the values were represented in Table 2. Here, one can notice that as a function of "Co" concentration or e/a ratio the martensitic transformation temperature also increases monotonously for all the processing conditions. However, upon heat treatment for all the conditions, the values suggest that there is

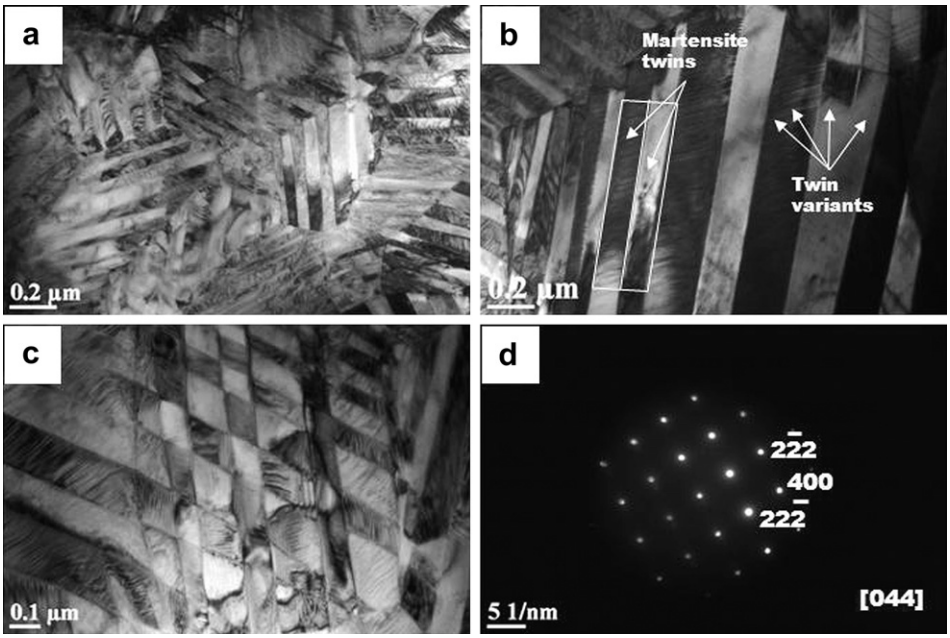

Fig. 3. TEM micrographs of $Ni_{50}Mn_{20}$ Co_8Ga_{25} alloy melt-spun at high wheel speed. (a) Bright field image showing martensite phase with twins (b) and (c) Bright field images of martensite phase at higher magnification (d) Corresponding SAED pattern taken from austenite phase indexed B2 atomic ordering along [044] zone axis.

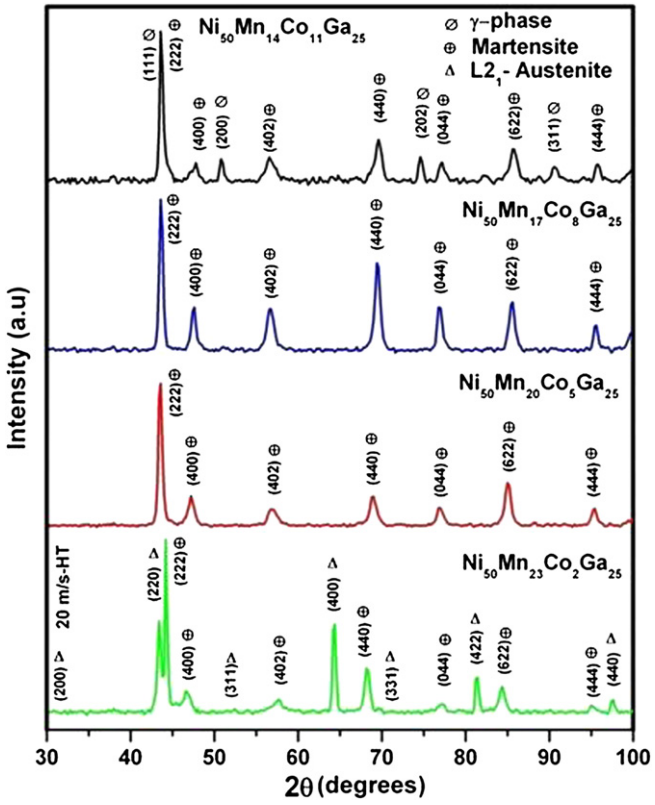

Fig. 4. XRD patterns of Ni_2(Mn,Co)Ga alloy samples melt-spun at low wheel speed and annealed. Patterns of samples with cobalt content of 2, 5, 8 and 11% are shown in increasing order from bottom to top.

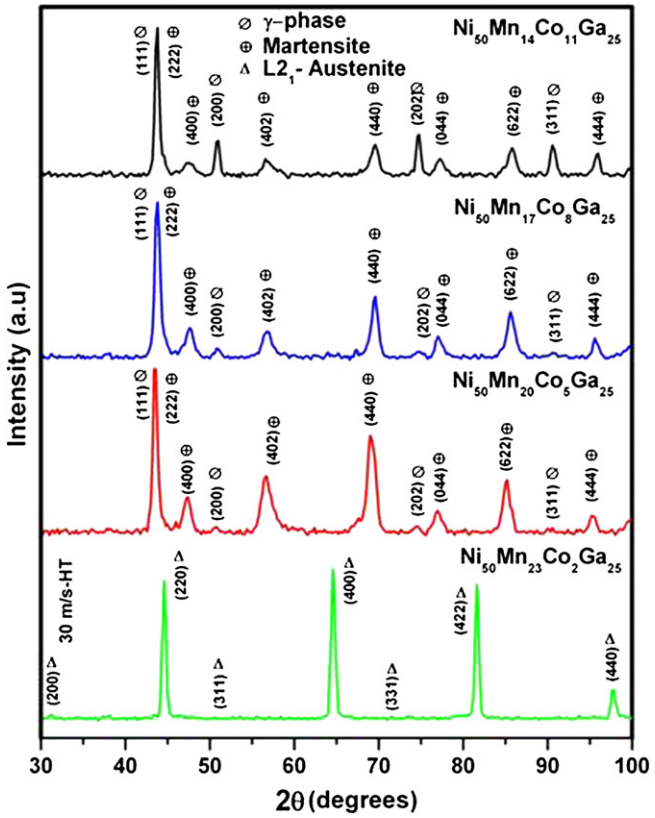

Fig. 5. XRD patterns of Ni_2(Mn,Co)Ga alloy alloy samples melt-spun at high wheel speed and annealed. Patterns of samples with cobalt content of 2, 5, 8 and 11% are shown in increasing order from bottom to top.

a drop in the martensitic transformation temperature compared with as-spun samples. The observed results are comparable with the available literature as shown in Fig. 3 in reference [32]. Similarly, Curie temperature vs. different processing conditions plot is given in Fig. 6c and also the values were indicated in Table 3. It is evident from the figure that Curie temperature is decreasing linearly as a function of cobalt content (or e/a ratio) for all the processing conditions. However, one can notice that decrease in the Curie temperature upon heat treatment for all the processing conditions except for certain the combination of high wheel speed and high cobalt content in the alloys. Composition dependence of Curie temperature in Ni_2MnGa Heusler alloys for comparison was shown in the study by Jin et al. [32].

4. Discussion

The 5at%-Co alloy exhibited 7 M or 14 Layered martensite. The formation of martensite in samples above certain cobalt content could be attributed to lattice strain that could bring the martensite transformation temperature to higher values. Precipitation of gamma phase in 11%-Co alloy upon annealing demonstrates that rapid solidification leads to extended solid solutions and metastable phase formation. Annealing at high temperature provides adequate activation to relax the microstructures and lead to higher chemical order ($L2_1$). Similar phase sequence observed in samples melt-spun at higher wheel speed but at lower cobalt content shows that both rapid solidification and higher alloying content lead to disorder in the as-spun samples.

Apart from the formation of austenite phase with B2 atomic ordering confirmed by TEM analysis, pre-martensitic tweed structures are also observed. The tweed structure appears in the characteristic cross-hatched pattern of contrast in bright field images. Earlier researchers observed “Tweed” patterns in electron micrographs in the vicinity of the transition temperature. The melt-spinning process results in higher degree of undercooling, which in turn could generate local fluctuations in the concentration. Also due to substitution of cobalt in place of manganese lattice distortion also aids in the disorder that is necessary for appearance of tweed contrasted regions as pre-martensite structures. Similar observations have been observed by Sanchez-Alarcos et al., by the addition of Co to Ni_2MnGa alloys, as it increases the quenched in defects, which in turn contributes to influence the transformation temperatures [17].

It is interesting to note that though non-modulated martensite is predominantly seen in samples containing higher cobalt content or melt-spun at higher wheel speed, one of the parametric combinations has resulted in modulated (7 M or 14 M layered) martensite in as-spun condition (5%-Co, low wheel speed). This sample too, upon annealing, results in non-modulated martensite. The study shows that rapid solidification of concentrated alloys of Ni_2MnGa has a direct role in determining the metastable microstructures, phase content and thus the martensite transformation temperature of the sample.

Precipitation of gamma phase in annealed 11%-Co alloy melt-spun at high wheel speed indicates upper limit of alloying content (8%-Co) to modify the martensite transformation temperature while keeping the microstructure single phase. Extended solid solution formation during rapid solidification and phase separation upon annealing is noticed in this alloy system as anticipated [33,34]. Increase of chemical order of austenite phase upon annealing and slow cooling is also noticed in Ni_2MnGa system as reported recently [35]. Moreover, a recent study by addition of Co to

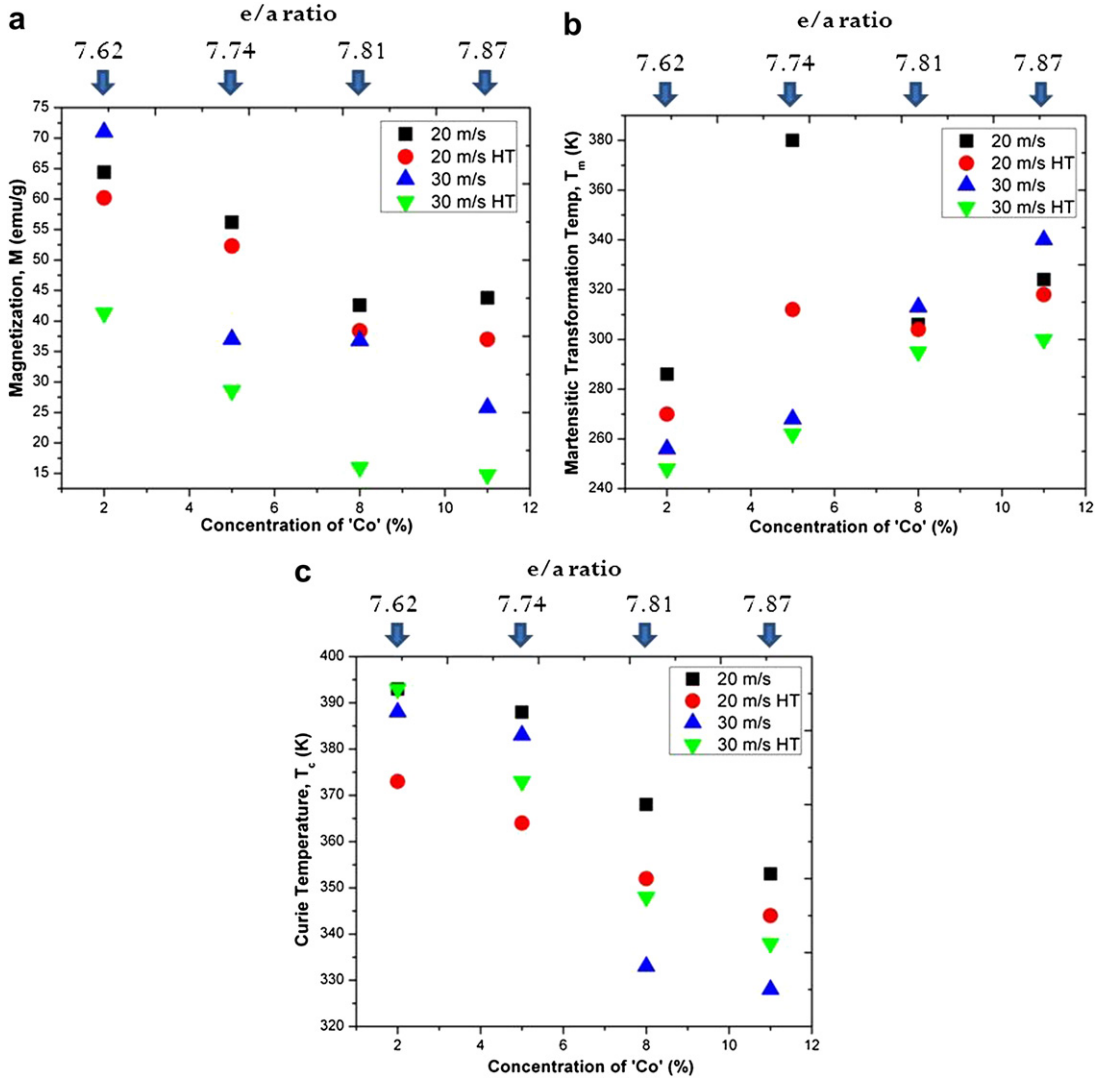

Fig. 6. Effect of 'Co' concentration and corresponding e/a ratio on (a) Saturation magnetization (b) Martensite transformation temperature and (c) Curie temperature of samples of Ni_2(Mn,Co)Ga processed in different conditions. The e/a values for corresponding average compositions are given in the *x*-axis at the top.

Ni_2MnGa system favors the formation of gamma phase and which enhances ductility at the expense of shape memory effect [12].

The results suggest that magnetic properties such as magnetization (Ms), martensitic transformation temperature (T_m) and Curie temperature (T_c) are sensitive to chemical composition and e/a ratio. One can notice that magnetization (Ms) values show composition dependence and linearly decrease as either cobalt content or e/a ratio increases. These results are comparable with literature [32] when the e/a ratio increase from 7.62 to 7.87. This is true for all the samples, irrespective of processing condition. However, the magnetization values decrease upon annealing compared to as-spun samples. This reason could be due to the formation of γ (gamma) phase upon annealing as noticed from XRD analysis. Although the magnetization values are decreasing, the martensitic transformation temperature increases as the cobalt content increases linearly, irrespective of processing condition. Earlier researchers [32,35] also observed linear dependence of martensitic transformation temperature (T_m) as the e/a ratio increases from 7.62 to 7.87. The increase in martensitic transformation temperature could be due to stabilizing martensite phase with increasing "Co" concentration. Minor decrease in the martensitic transformation temperature for annealed samples could be due to lattice relaxation and evolution of γ (gamma) phase upon annealing.

Table 1
Saturation magnetization values of Co-substituted Ni_2(Mn,Co)Ga melt-spun ribbons with different processing conditions.

Co- content	Magnetization Ms (emu/g)			
	20 m/s	20 m/s annealed	30 m/s	30 m/s annealed
2 at. %	64.4	60	71.0	41.3
5 at. %	56.2	52	37.0	28.6
8 at. %	42.6	38	36.8	16.0
11 at.%	43.8	37	25.8	14.8

Table 2
Martensitic transformation temperature (T_m) values of Co-substituted Ni_2(Mn,Co)Ga melt-spun ribbons with different processing conditions.

Co- content	Martenstic transformation temperature, T_m(K)			
	20 m/s	20 m/s annealed	30 m/s	30 m/s annealed
2 at.%	286	270	256	248
5 at.%	380	312	268	262
8 at.%	306	304	313	295
11 at.%	324	318	340	300

Table 3
Curie temperature, T_c (K) values of Co-substituted Ni_2(Mn,Co)Ga melt-spun ribbons with different processing conditions.

Co- content	Curie temperature, T_c(K)			
	20 m/s	20 m/s annealed	30 m/s	30 m/s annealed
2 at.%	393	373	388	393
5 at.%	388	364	383	373
8 at.%	368	352	333	348
11 at.%	353	344	328	338

Curie temperature also shows decreasing trend linearly with composition. Upon annealing there is marginal decrease in the Curie temperature and it could be due to formation phase mixture (such as austenite + martensite and martensite + gamma). Although there is a drawback owing to presence of γ (gamma) phase on the magnetic properties, it is known to impart ductility and toughness to the Ni_2(Mn,Co)Ga Heusler alloys [33]. This study shows that a combination of rapid solidification to enhance solid solution limits, annealing to increase chemical order or precipitation of gamma phase could be used to tune both ductility and magnetic properties to a desired combination. In the present study, desirable magnetic properties are obtained for room temperature applications for samples containing higher cobalt content (8, 11%) in the $Ni_{50}Mn_{(25-x)}Co_xGa_{25}$ Heusler alloys.

5. Conclusions

1. In the Ni_2(Mn,Co)Ga Heusler alloy ribbons melt-spun at wheel speeds of 20 m/s and 30 m/s, martensite phase stabilizes at higher "Co" concentrations (8%-Co, 11%-Co).
2. The 5%-Co alloy sample melt-spun at low wheel speed showed presence of modulated (seven layered or 14 M) martensite phase.
3. γ (gamma) phase stabilizes upon heat treatment (annealing at 1273 K) for ribbons synthesized by melt spinning at higher wheel speed and higher cobalt content.
4. Magnetization (M_s), Martensite transformation temperature (T_m) and Curie temperature (T_c) shows a fairly linear trend with increasing cobalt content
5. Desirable combination of properties are achieved for room temperature applications for 5%-Co alloy sample melt-spun at low wheel speed as follows:
   a) As-spun condition: M_s: 56.2 emu/gm; T_m: 380 K; T_c: 388 K.
   b) Annealed condition: M_s: 52 emu/gm; T_m: 312 K; T_c: 364 K.

Acknowledgments

The authors thank M. Srinivas and Dr. Bhaskar Majumdar, Defense Metallurgical Research Laboratory for experimental facilities and useful discussions.

References

[1] Ullakko K, Huang JK, Kantner C, Kokorin VV, O'Handley RC. Applied Physics Letters 1996;69:1966–8.
[2] Richard ML, Feuchtwanger J, Allen SM, O'handley RC, Lazpita P, Barandiaran JM, et al. Phil Mag 2007;87:3437–47.
[3] Ducher R, Kainuma R, Ohnuma I, Ishida K. Journal of Alloys and Compounds 2007;437:93–101.
[4] Ducher R, Kainuma R, Ishida K. Journal of Alloys and Compounds 2008;466: 208–13.
[5] Oikawa K, Omori T, Sutou T, Morito H, Kainuma R, Ishida K. Metallurgical and Materials Transactions A 2007;38A:767–76.
[6] Oikawa K, Ota K, Imano Y, Omori T, Kainuma R, Ishida K. Journal of Phase Equilibria and Diffusion 2006;27:75–82.
[7] Omori T, Kamiya N, Sutou Y, Oikawa K, Kainuma R, Ishida K. Materials Science and Engineering A 2004;378:403–8.
[8] Liu J, Xia Mingxu, Huang Yanlu, Zheng Hongxing, Li Jianguo. Journal of Alloys and Compounds 2006;417:96–9.
[9] Wang HB, Chen F, Gao ZY, Cai W, Zhao LC. Materials Science and Engineering A 2006;438–440:990–3.
[10] Soto D, Hernández Francisco Alvarado, Krenke Thorsten, Flores-Zúñiga Horacio, Moya Xavier, Mañosa Lluís, et al. Physical Review B 2008;77: 184103.
[11] Fabbrici S, Kamarad J, Arnold Z, et al. Acta Materialia 2011;59:412–9.
[12] SY Ma YQ, Jiang HF, et al. Intermetallics 2011;19:225–8.
[13] Soto-Parra DE, Moya X, Manosa L, et al. Philosophical Magazine 2010;90: 2771–92.
[14] Fabbrici S, Albertini F, Paoluzi A, et al. Applied Physics Letters 2009;95: 022508.
[15] Chernenko VA, Oikawa K, Chmielus M, et al. Journal of Materials Engineering and Performance 2009;18:548–53.
[16] Sanchez-Alarcos V, Perez-Landazabal JI, Recarte V, et al. Acta Materialia 2008; 56:5370–6.
[17] Sanchez-Alarcos V, Perez-Landazabal JI, Recarte V. Materials Science and Engineering A 2008;481:293–7.
[18] Cong DY, Wang S, Wang YD, et al. Materials Science and Engineering A 2008; 473:213–8.
[19] Prasad RVS, Phanikumar G. Journal of Material Science 2009;44:2553–9.
[20] Prasad RVS, Phanikumar G. Materials Science Forum 2010;649:35–40.
[21] Prasad RVS, Raja M, Phanikumar G. Advanced Materials Research 2009;74: 215–8.
[22] Prasad RVS, Phanikumar G. Intermetallics 2011;19:1705–10.
[23] Pons J, Chernenko VA, Santamarta R, Cesari E. Acta Materialia 2000;48: 3027–38.
[24] Robertson IM, Wayman CM. Metallography 1984;17:149–63.
[25] Shapiro SM, Larese JZ, Noda Y, Moss SC, Tanner LE. Physical Review Letters 1986;57:3199–202.
[26] Akahoshi D, Hatakeyama R, Nagao M, Asaka T, Matsui Y, Kuwahara H. Physical Review B 2008;77:054404.
[27] Bysakh S, Das PK, Chattopadhyay K. Materials Science and Engineering A 2001;304–306:608–11.
[28] Khachaturyan AG, Shapiro SM, Semenovskaya S. Physical Review B 1991;43: 10832–43.
[29] Chernenko VA, Pons J, Seguı C, Cesari E. Acta Materialia 2002;50:53–60.
[30] Kartha S, Krumhansl JA, Sethna JP, Wickham LK. Physical Review B 1995;52: 803–21.
[31] Kartha S, Castan. T, Krumhansl JA, Sethna JP. Physical Review Letters 1991;67: 3630–3.
[32] Jin X, Marioni M, Bono D, Allen SM, O'Handley RC, Hsu TY. Journal of Applied Physics 2002;91:8222–4.
[33] Ma Y, Yang Shuiyuan, Liu Yong, Liu Xingjun. Acta Materialia 2009;57: 3232–41.
[34] Overholser RW, Wuttig M, Neumann DD. Scripta Materialia 1999;40: 1095–102.
[35] Sanchez-Alarcos V, Recarte V, Perez-Landazabal VI, Cuello GJ. Acta Materialia 2007;55:3883–9.